Talanta 222 (2021) 121516

Contents lists available at ScienceDirect

Talanta

journal homepage: www.elsevier.com/locate/talanta

Immuno-cytometric detection of circulating cell free methylated DNA, post-translationally modified histones and micro RNAs using semi-conducting nanocrystals

Ruchita Shandilya [a,1], Neha Bunkar [a,1], Roshani Kumari [a], Arpit Bhargava [a], Koel Chaudhury [b], Irina Yu Goryacheva [c], Pradyumna Kumar Mishra [a,*]

[a] Department of Molecular Biology, ICMR-National Institute for Research in Environmental Health, Bhopal, India
[b] School of Medical Science & Technology, Indian Institute of Technology, Kharagpur, India
[c] Department of General and Inorganic Chemistry, Saratov State University, Saratov, Russia

ARTICLE INFO

Keywords:
Circulating epigenomic signatures
Circulating nucleic acids
Nano-biosensor
Immuno assay
Translational research

ABSTRACT

The diagnostic potential of cell free epigenomic signatures is largely driven by the fact that manifold quantities of methylated DNA, post-translationally modified histones and micro RNAs are released into systemic circulation in various non-communicable diseases. However, the time-consuming and specificity-related complications of conventional analytical procedures necessitate the development of a method which is rapid, selective and sensitive in nature. The present work illustrates a novel; prompt; "mix and measure" cytometric-based nano-biosensing system that offers direct quantification of cell-free circulating (*ccf*) epigenomic signatures (methylated *ccf*-DNA, tri-methylated histone H3 at lysine {4, 9, 27 & 36} and argonaute 2 protein-bound *ccf*-micro RNAs) using triple nano-assemblies in a single tube format. Each assembly with unique structural and spectral properties comprised of n-type semiconducting nanocrystals conjugated to a specific monoclonal antibody. Our results suggested that the developed combinatorial approach may offer simultaneous detection of three distinct yet biologically interrelated signatures with high selectivity and sensitivity using flow cytometry and fluorometry in the enriched and test samples. The proposed novel nano-assembly based detection system has a considerable potential of emerging as a minimal invasive easy-to-use method that could possibly permit real-time, rapid and reproducible monitoring of epigenomic markers in clinical and field settings.

1. Introduction

Over the past few years, nanoscience in combination with sensing technology have paved the way for development of miniaturized and simplified frameworks termed as nano-biosensors [1–3]. The progression of these nano-assemblies in healthcare has led to the development of novel diagnostic strategies that could provide precise and rapid disease detection. Advancements in nano-biosensing have promoted the development of frameworks that assimilate several exploratory methodologies into a single portable unit to provide precise, sensitive and prompt detection of the circulating biological markers [4–6]. Among the biosensors, optical nano-sensors have attracted significant attention in the recent past as they offer high sensitivity and selectivity, improved signal-to-noise ratio, better performance flexibility in construction as per the requirement and portability [7,8]. The diagnostic module in the optical miniaturized framework involves detection of change in the

Abbreviations: Ab, Antibody; AGO2, argonaute 2 protein; cDNA, complementary DNA; *ccf*, circulating cell free; Ct, cycle threshold; dCt, delta Ct; 5-mC, 5-Methylcytosine; *ccf*-DNA, circulating cell-free DNA; *ccf*-miRs, circulating cell-free miRNAs; EDC, (1-ethyl-3-[3-dimethylaminopropyl]carbodiimide hydrochloride); ELISA, enzyme linked immunosorbent assay; HRP, horseradish peroxidise; miRNA, microRNA; MSP, methyl specific PCR; NHS, N-hydroxysuccinimide; NFW, nuclease-free water; PCR, polymerase chain reaction; qPCR, quantitative polymerase chain reaction; QDs, quantum dots; QD-Ab, quantum dot-antibody conjugate; QD-525-Ab, conjugate of QD-525 and antibodies specific for tri-methylated histone H3 at lysine {4, 9, 27 & 36} residues; QD-625-Ab, complex of QD-625 with the methylated *ccf*-DNA specific antibodies; QD-705-Ab, conjugate of QD-705 with anti-AGO2 antibodies; TAE, Tris-acetate-EDTA.

* Corresponding author. Department of Molecular Biology, ICMR-National Institute for Research in Environmental Health, Kamla Nehru Hospital Building, (Gandhi Medical College Campus), Bhopal, MP, 462001, India.
E-mail address: pkm_8bh@yahoo.co.uk (P.K. Mishra).
[1] Authors contributed equally.

https://doi.org/10.1016/j.talanta.2020.121516
Received 25 March 2020; Received in revised form 17 July 2020; Accepted 22 July 2020
Available online 13 August 2020

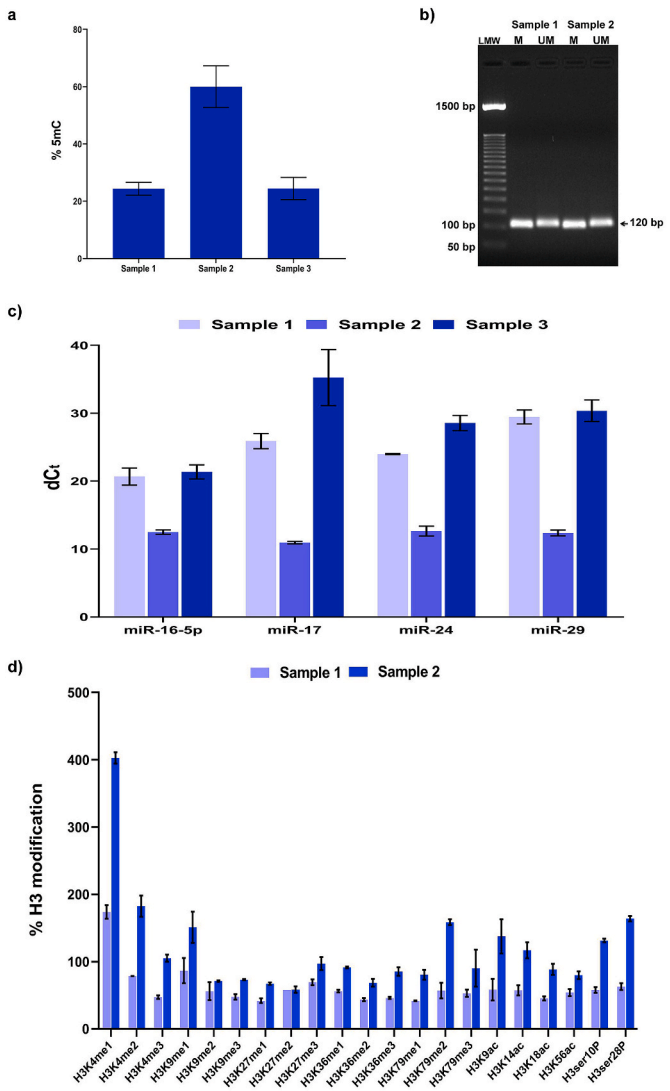

Fig. 1. Figure showing the characterization of circulating epigenomic signatures i.e. (a) global DNA methylation (5-mC%) levels (n = 3) (b) representative gel image of methylated (100 bp) and un-methylated (120 bp) *ccf*-DNA (n = 2), LMW; low molecular weight marker, M; methylated, UM; unmethylated (c) expression patterns of four AGO-bound *ccf*-miRs (n = 3) and (d) levels of histone H3 modifications (n = 3). The bars represent mean ± SE values, and $p \leq 0.05$ was considered statistically significant.

absorption or, more often, the emission of light, in response to precise identification of the respective analytes [9]. Semiconducting colloidal nanocrystals, often termed as quantum dots (QDs), reserves an imperative spot in optical sensing research owing to their emerging use in detection of biological entities over the past decades [10]. QDs are zero dimensional nanoparticles that exhibit size-dependent luminescence and offer a variety of advantages ranging from size tunability; large band-gap; small Stokes shift; strong quantum confinement; intense and long-lasting luminescence; high quantum yield; and resistance to photo-bleaching in comparison to conventional organic fluorophores. In addition, the ease of surface modification provides other benefits such as instigation of desired physico-chemical properties and attachment of bio-recognition elements. On account of these exceptional properties, the recent years have witnessed a substantial increase in the use of QDs to develop multi-element nano-assemblies for concurrent optical biosensing applications [10–12].

Of late, with the progression of diagnostic technologies, an increase in the use liquid biopsy method for early screening of disease associated risk factors has been observed. The use of circulating cell free (*ccf*) nucleic acids in liquid biopsy is largely motivated by the fact that the human body generates 10–100 billion cells each day and an equal amount of cells undergo apoptosis to maintain cellular homeostasis that results in the release of their genetic materials in peripheral milieu [12–16]. The levels of such circulating moieties exist at varying concentrations ranging from scantly detectable to few micrograms per liter, with significant elevated levels in diseased conditions like cancer, sepsis, diabetes, renal failure and auto-immune disorders [13]. These differential levels could provide a detailed insight of altered biological processes which in turn might aid in early identification of the occurrence and progression of a disease at various stages [17–22]. In the present scenario, liquid biopsy in combination with optical nanosensors has emerged as a research hotspot, offering potential benefits over the existing methodologies. The combinatorial approach possesses the capability to generate rapid medical conclusions that shall help in early diagnosis and timely commencement of the therapy [23–26]. This may not only result in significant reduction of disease severity but also increase the probability of patient's survival [27–30].

Considering the advantage of the multiplexed approach into account, we aimed to develop a triple quantum dot-antibody (QD-Ab) based immuno-detection assay for the rapid and simultaneous detection of three *ccf* epigenomic markers, which include methylated *ccf*-DNA, trimethylated histone H3 at lysine {4, 9, 27 & 36} and argonaute 2 protein (AGO2)-bound *ccf*-miRs in a single tube format. The single tube format refers to the cocktail of different color-coded triple immunoconjugates that could simultaneously determine the aforementioned triple signatures in the same sample owing to their respective specificity, without any spectral overlapping or interference in the analysis. The method may serve as a novel "mix and measure" flow cytometry based immunoassay that involves development of three different QD-Ab immuno-conjugates for detection of the three different circulating signatures, emphasizing its clinical application in disease diagnosis.

2. Materials and methods

2.1. Buffers and reagents

QDs (Qdots™ 525, 625 and 705), EDC (1-ethyl-3-[3-dimethylaminopropyl] carbodiimide hydrochloride), NHS (N-hydroxysuccinimide), and anti-AGO2 monoclonal Ab were procured from the ThermoFisher Scientific (Waltham, MA, USA). 5-Methylcytosine (5-mC), Tri-Methyl-Histone H3 (Lys4) Rabbit monoclonal Ab, Tri-Methyl-Histone H3 (Lys9) Rabbit monoclonal Ab, Tri-Methyl-Histone H3 (Lys27) Rabbit monoclonal Ab and Tri-Methyl-Histone H3 (Lys36) Rabbit monoclonal Ab were purchased from the Cell Signaling Technology, Inc. (Danvers, MA, USA). Sodium phosphate monobasic anhydrous, sodium phosphate dibasic anhydrous and syringe-driven filters with pore size of 0.22 μm and 0.45 μm were obtained from HiMedia Laboratories (Mumbai, MH, India). To assess electrophoretic mobility of QDs, agarose was bought from Lonza Inc., (Basel, Switzerland), while 1X TAE buffer and 6X gel loading buffer were purchased from HiMedia Laboratories (Mumbai, MH, India). The visual tracking of differential migration during electrophoresis was done by using SYBR® Safe DNA gel stain procured from the ThermoFisher Scientific (Waltham, MA, USA). For isolation of circulating nucleic acids, Nucleospin® miRNA plasma kit from Macherey-Nagel, Duren, Germany and QIAamp® Circulating Nucleic Acid Kit from Qiagen Hilden, Germany were used. Poly-A tailing kit was procured from Invitrogen Thermofisher Scientific, Waltham, MA, USA. PrimeScript 1st strand cDNA Synthesis was bought from Takara Bio Inc. (Shiga, Japan). GoTaq qPCR master mix was obtained from Promega Corporation (Madison, WI, USA). EpiQuik™ Total Histone extraction kit and EpiQuik™ Histone H3 modification multiplex assay kit (colorimetric) were bought from Epigentek Group Inc., (Farmingdale, NY, USA). 5-mC DNA ELISA kit was procured from Zymo Research (Irvine, California, USA). Histone assay control protein (100 μg/mL) from

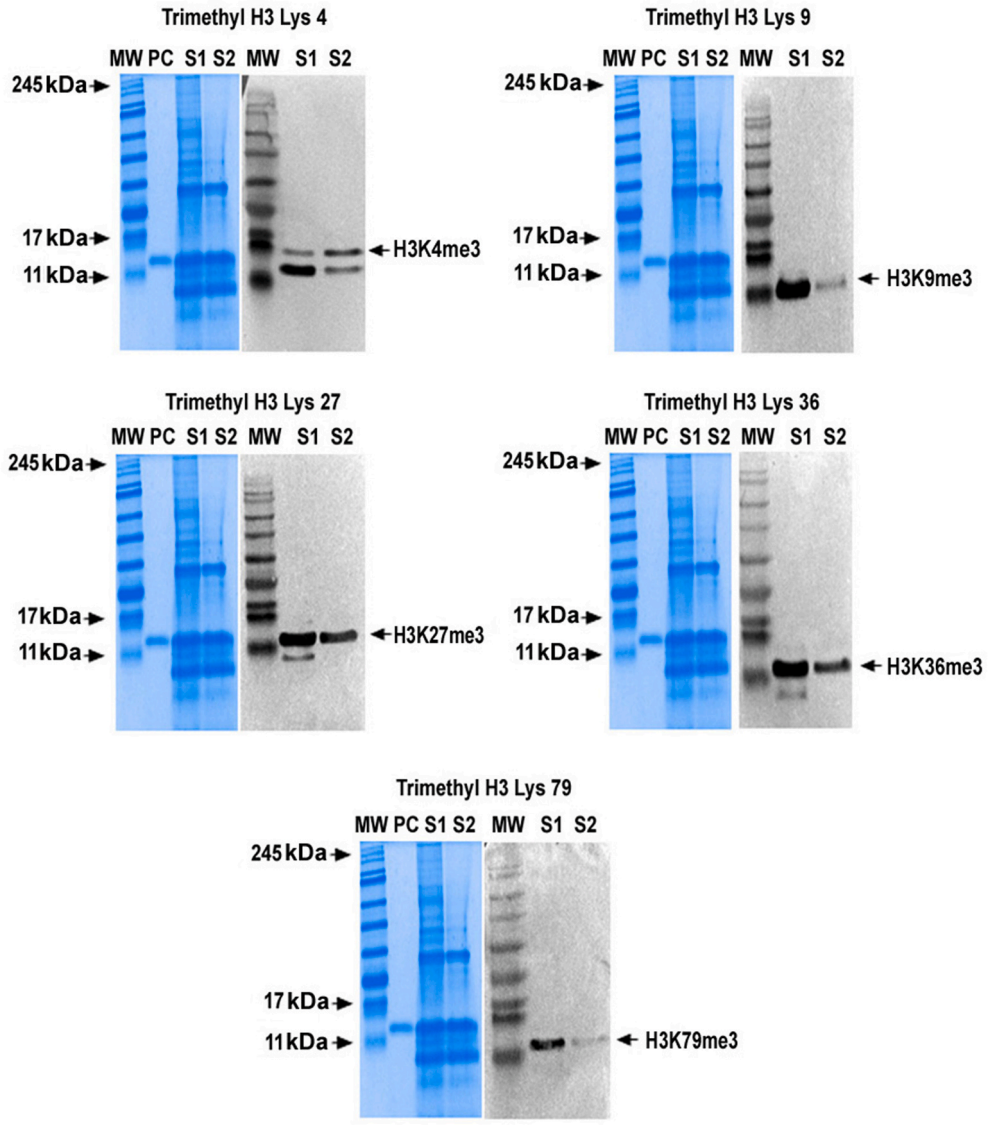

Fig. 2. Representative blot images showing the profile histone (H3) modifications in two samples. MW: molecular weight, PC: positive control, S1; sample 1, S2: sample 2. H3K4me3; trimethylated histone H3 at lysine 4, H3K9me3; trimethylated histone H3 at lysine 9, H3K27me3; trimethylated histone H3 at lysine 27, H3K36me3; trimethylated histone H3 at lysine 36, H3K79me3; trimethylated histone H3 at lysine 79.

Epigentek Group Inc., (Farmingdale, NY, USA) and methylated control DNA (50 ng/μL) from Sigma Aldrich, St. Louis, Missouri, USA were used as reference controls. The bovine serum albumin (BSA) used for preparation of the blocking buffer was purchased from HiMedia Laboratories, Mumbai, MH, India. Nuclease free water was bought from HiMedia Laboratories (Mumbai, MH, India).

2.2. Triple QD-Ab conjugation

The work involved preparation of three different QD-Ab immuno-conjugates, which served as reporter systems with unique structural, molecular and optical characteristics. The first immuno-complex was prepared by conjugating QD-525 with monoclonal Abs specific to trimethylated histone H3 at lysine {4, 9, 27 & 36} residues (QD-525-Ab), while the association of QD-625 with the monoclonal Abs possessing high affinity towards methylated *ccf*-DNA (QD-625-Ab) resulted in the preparation of the second immuno-conjugate. The third composite was prepared by coupling QD-705 with anti-AGO2 polyclonal Abs (QD-705-Ab) specific for AGO2- protein bound *ccf*-miRs.

The conjugation of surface carboxyl groups comprising QDs (525, 625 and 705) with amine groups of the respective Abs was performed using carbodiimide coupling protocol as described in Shandilya et al., 2020 [3]. The conjugation was promoted by cross-linkers EDC and NHS (Fig. S1). Prior to coupling, 10 μL of solution (8 μM) of each QD (525, 625 and 705) comprising 4.8×10^{13} particles were re-suspended in 250 μL phosphate buffer (20 mM, pH 7.4). This was followed by pre-activation of QDs with freshly prepared EDC and NHS (25 μL of each 10 mg/mL solution) for 20 min. After incubation, appropriate volume of the respective Abs was added and the complex was incubated at room temperature for 30 min. Following incubation, a second aliquot of EDC and NHS (25 μL of each solution) was added for the enhancement of conjugation efficiency and incubated overnight at 4 °C. The detection capability of the prepared immuno-conjugates was assessed in enriched samples and in plasma.

2.3. Evaluation of the QD-Ab immuno-conjugates

The QD-Ab conjugation was confirmed using electrophoretic mobility assay. For this, 10 μL of three immuno-sensing conjugates (QD-525-Ab; QD-625-Ab and QD-705-Ab) and 2 μL of un-conjugated QDs

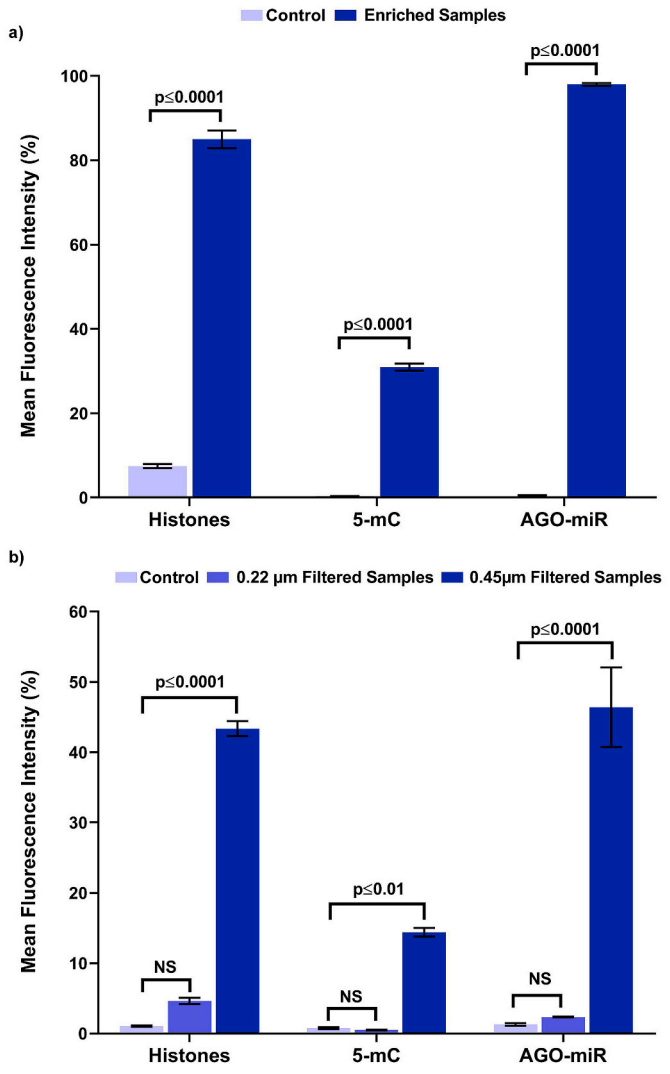

Fig. 3. Graphs illustrating the comparative flow cytometric analysis (n = 3) of (a) samples enriched in histones, *ccf*-DNA and *ccf*-miRs and (b) samples obtained by 0.22 µm and 0.45 µm filtration. The Ab conjugated QDs were used as controls and the data is expressed as mean ± SE. $p \leq 0.05$ was considered statistically significant.

solution (525, 625 and 705) were mixed with 1X TAE buffer and 2 µL 6X gel loading dye. The mixtures were loaded in the 1% agarose gel in separate lanes and the electrophoretic mobility was assessed at 100 V for 20 min in 1X TAE buffer. The movement of the QD-Ab conjugates with respect to un-conjugated QDs was analyzed using Gel Doc™ XR + molecular imager (Bio-Rad, USA) [31].

2.4. Assessment of the detection capability in enriched samples

The detection capability of the prepared immuno-conjugates was analyzed using flow cytometry in target-enriched samples. The enriched samples comprised of histone, *ccf*-DNA and *ccf*-miRs isolated as per the manufacturer's instructions. For the detection, 30 µL of each QD-Ab conjugate was added to 100 ng of previously isolated histone, *ccf*-DNA and *ccf*-miRs in separate tubes. Histones and *ccf*-DNA were mixed with QD-525-Ab and QD-625-Ab respectively, while the isolated *ccf*-miRs were added to the tube of QD-705-Ab conjugates. The volume of each tube was make-up to 300 µL by adding nuclease-free water (NFW) and the analysis was performed on flow cytometer (Attune NXT, ThermoFisher Scientific, USA). All the measurements were recorded with respect to negative controls consisting of Ab conjugated QDs. The procedure was performed in triplicates and compared for reproducibility of detection of the respective analytes.

2.5. Validation of the detection in plasma

Real-time detection of the levels of three epigenomic signatures was performed directly in plasma using flow cytometry. For this, plasma samples were initially subjected to 0.22 µm filtration to obtain clear plasma devoid of any large sized genetic debris and filtration by 0.45 µm filters to remove mesechymal cells and cellular debris including extracellular microvesicles, lipid rafts, apoptotic/necrotic bodies and exosomes, conserving the nucleosomes (DNA-histone complexes), methylated *ccf*-DNA and AGO2-bound *ccf*-miRs. Later, 300 µL of filtered plasma samples were added in three clean micro-centrifuge tubes. To this, 30 µL of each QD-Ab conjugates were added and vortexed. The prepared mixtures were acquired by flow cytometry and the data for three sets of replicates were analyzed.

2.6. Sensitive recognition of triple epigenomic signatures in circulation

The sensitivity of the immuno-sensing semi-conducting complexes was assessed as a measure of their ability to precisely capture trimethylated histones, methylated DNA and AGO2 bound miRNAs in circulation at differential levels. Isolated plasma samples were subjected to high speed centrifugation followed by double filtration by 0.22 µm filters to completely remove the microvesicles, lipid rafts, protein bound molecules, apoptotic/necrotic bodies and exosomes including large genetic debris. The obtained clear plasma samples (300 µL each) were added to a known concentration (10 ng–0.001 ng) of reference controls (H3 histones, methylated DNA and PCR products of AGO2-bound *ccf*-miRs). Subsequently, 30 µL of QD- Ab conjugates were added and subjected for flow cytometric acquisition and analysis. The same set of samples was also analyzed by fluorometry to confirm our flow cytometry results. The fluorometric measurements were done by using Spark® multimode microplate reader (TECAN, Seestrasse 103, Männedorf, Switzerland).

2.7. Concurrent detection of modified histones, methylated ccf-DNA and AGO-2 bound ccf-miRs

The ability of triple immuno-sensing nanocrystals to simultaneously detect respective epigenomic markers in the presence of other biomolecules was assessed in the aforementioned plasma samples using flow cytometry. For concurrent detection in a single tube format, samples enriched in target signatures were pooled (histones: methylated *ccf*-DNA and histones: AGO2 bound *ccf*-miRs) and a cocktail of QD-Ab immuno-conjugates (QD-525-Ab: QD-625-Ab and QD-525-Ab: QD-705-Ab) was added. The analysis was performed through flow cytometry using Ab conjugated QDs as negative controls.

2.8. Isolation and characterization of histones, ccf-DNA and ccf-miRNA

As a proof of principle that epigenomic signatures circulate at differential levels in healthy and diseased states, circulating modified histones, methylated *ccf*-DNA and AGO-2 bound *ccf*-miRs were characterized using PCR, Western blot and ELISA based approaches. Histones, *ccf*-DNA and *ccf*-miRNAs were isolated as per the direction of the standardized protocols of EpiQuik™ total histone extraction kit, QIAamp® circulating nucleic acid kit, and Nucleospin® miRNA plasma kit, respectively. For the quantification of multiple histone H3 modifications, a plex of twenty one (21) modified histone H3 patterns was analyzed by a sandwiched ELISA method using EpiQuik™ Histone H3 modification kit. Western blot analysis of H3 modifications was performed as per standard protocol discussed elsewhere using appropriate set of Abs. Status of DNA methylation was assessed using 5-mC DNA ELISA kit using Spark® multimode microplate reader (TECAN,

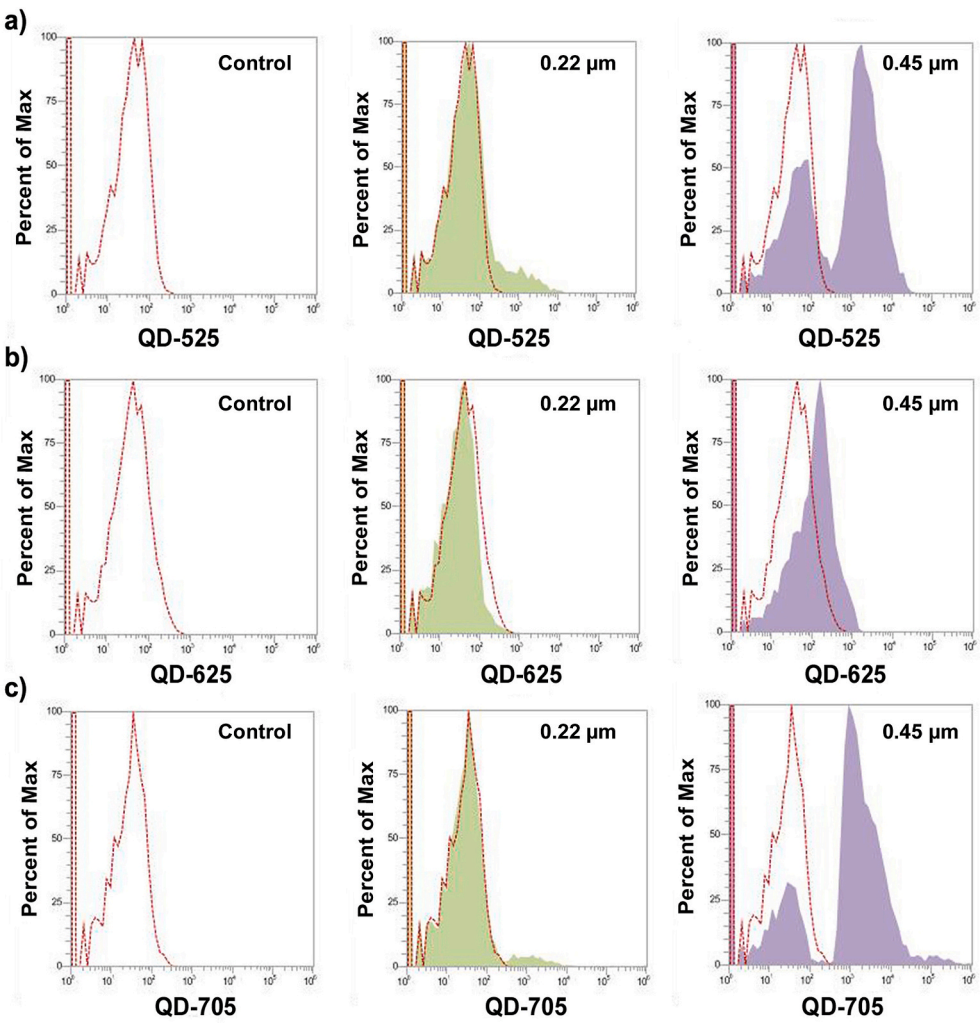

Fig. 4. Representative flow cytometry histograms of the QD-Ab immuno-conjugates validating their ability to detect target analytes (H3 histones, methylated *ccf*-DNA and AGO2 bound *ccf*-miRs) in plasma samples filtered through 0.22 µm and 0.45 µm filters. The x axis of the histogram represents the observed fluorescence, while the y axis shows the normalized values of absolute count to the 100% of total. The Ab conjugated QDs (red) were used as controls and the shift in peak indicates an increase in fluorescence upon target detection. (For interpretation of the references to color in this figure legend, the reader is referred to the Web version of this article.)

Seestrasse 103, Männedorf, Switzerland), while methylation-specific PCR (MSP) was performed to check the levels of global DNA methylation. The miRNA expression analysis was performed using Insta Q96™ Real-time PCR (Himedia Laboratories, Mumbai, MH, India). In brief, previously isolated *ccf*-miRs were quantified and subjected to poly-A sequence attachment followed by cDNA synthesis using the standardized kit protocol. The cDNA was then amplified using GoTaq qPCR Master Mix and miR-specific primers (a plex of four *ccf*-miRs) as discussed elsewhere. The Ct values were recorded and dCt was calculated for the assessment of aberration in the expression patterns of *ccf*-miRs [3,32].

2.9. Statistical analysis

All the results were expressed as mean ± standard error (n = 3). Statistical analysis was performed using the GraphPad Prism Version 5.03 (GraphPad Software, San Diego, CA, USA). The statistical differences were computed using one-way or two-way analysis of variance. *P* values ≤ 0.05 was considered significant.

3. Results and discussion

Epigenetic modifications including DNA methylation, histone tail modifications and alteration in the miRNA expressions play a crucial role in maintenance of a vital equilibrium between apoptosis, proliferation, regeneration and repair [33–35]. Since these signatures circulate at abnormal levels during different pathological conditions, concurrent profiling through novel sensoric methods could generate an epigenome-wide analytical landscape to provide essential insights of an individual's disease status. In our study, the characterization of circulating epigenomic signatures showed that the levels of the global DNA methylation, miRNA expression profile and histone modification pattern varies among the individual samples (Figs. 1 and 2).

Keeping the idea of the diagnostic applicability of circulating epigenomic signatures, the present work describes a novel immuno-sensing assay for simultaneous detection of methylated DNA, modified histone protein and AGO2-bound miRNA using flow cytometry. The developed method offers a simple, economical and high-throughput strategy for the efficient detection of all the aforementioned molecular species in a single tube. In order to detect the above molecular markers, tri-color coded reporter systems were prepared by conjugating QDs exhibiting green (QD-525), orange (QD-625) and far red (QD-705) fluorescence with specific Abs using carbodiimide chemistry. The prepared immuno-conjugates offer a unique combination of reporter and recognition elements forming a triple nano-biosensing cocktail for the real-time detection of the respective epigenomic signatures. The precise identification was highly facilitated by the size dependent spectral properties of the QDs (525, 625 and 705) and specific affinity of the paratopes of Abs towards their potential epitopes on the respective analytes [3,36]. The Ab structure is usually "Y" shaped comprising of two F(ab) regions and one Fc region. The F(ab) regions consist of antigen binding domains that significantly correlates with the antigen-binding capacity. While, the Fc

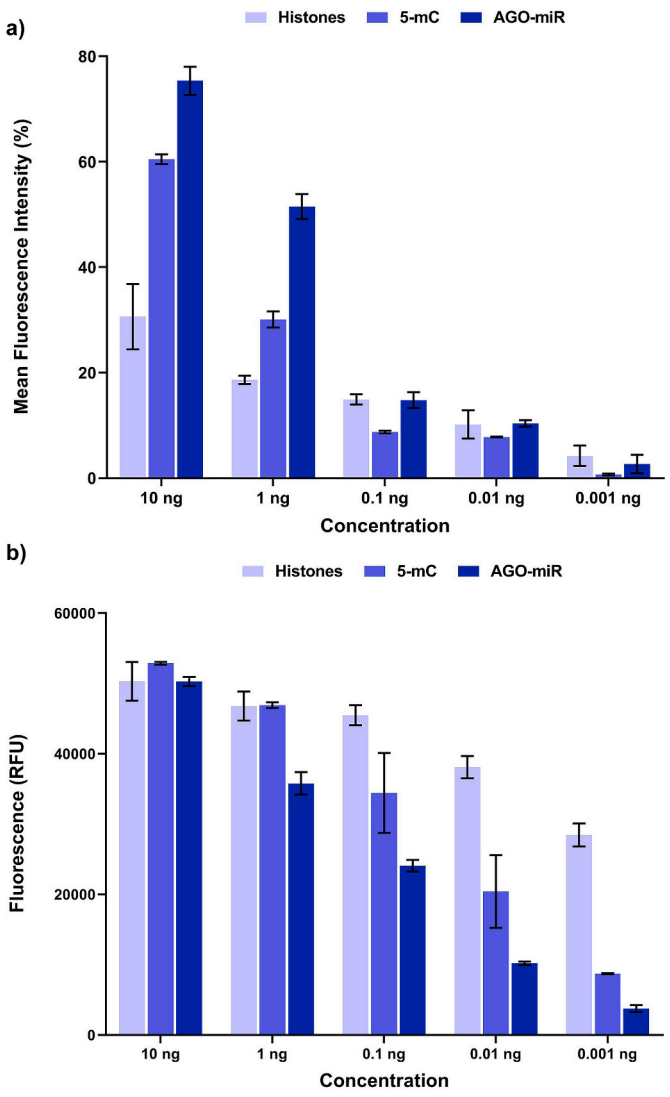

Fig. 5. Figure showing the ability of QD-Ab immuno-conjugates to precisely capture target analytes in plasma samples spiked with reference controls (H3 histones, methylated *ccf*-DNA and PCR products of AGO2-bound *ccf*-miRs) at the concentration ranging from 10 ng to 0.001 ng by flow cytometry (a) and fluorometry (b). The data is expressed as mean ± SE values (n = 3).

region contains primary amine groups on the lysine residues that serve as attractive sites for conjugation with the carboxyl groups of QDs. Thus, appropriate surface coverage and orientation of the immobilized Ab governs the sensitivity and analytical performance of the developed nano-conjugates. It is important to note that the pH of the reaction herein, plays a crucial role to control the orientation of the adsorbed Ab. At pH 7.3–7.5, the basic amino acid residues residing at the surface were protonated to a greater extent, thereby giving rise to localized regions of positive charge with maximum antigen-binding activity [37–39].

In view of the conjugation chemistry, the total number of Abs attached to a single QD was calculated according to the method described by Pathak et al., 2007 [40]. It was found that in QD-525-Ab complex, about 1.4 molecules of Abs were conjugated to each QD-525, whereas, approximately, 4.2 molecules of Abs were attached to a single QD-625 particle in the QD-625-Ab conjugate. Similarly in the QD-705-Ab conjugate, around 3.2 molecules of Abs were found to be attached with every QD-705 particle. Moreover, the efficient QD-Ab conjugation was confirmed by the observed electrophoretic mobility of QDs which primarily depends on their size and net charge. The movement of QD-Ab immuno-conjugates was found to be highly restricted due to reduction in the surface negative charge and increase in the overall size, while in contrast, the smaller un-conjugated QDs showed rapid migration within the gel (Fig. S2).

Following optimum conjugation, we checked the detection capability of the prepared immuno-conjugates (QD-525-Ab, QD-625-Ab and QD-705-Ab) in samples enriched in histones, *ccf*-DNA and *ccf*-miRs using flow cytometry. The detection was performed using excitation wavelength of 488 nm and 561 nm, while the observations were made in BL-1, BL-2, and YL-3 channels equipped with 530/30, 590/40, and 695/40 bandpass filters, respectively. The Ab conjugated QDs (without sample) were used as negative controls for comparative analysis. It was observed that all three complexes, when incubated with enriched samples show significantly higher fluorescence thereby suggesting their ability to detect the respective targets. The results evidenced that the levels of trimethylated histones H3, methylated *ccf*-DNA and AGO2-bound *ccf*-miRs were precisely recognized by the prepared conjugates, i.e. QD-525-Ab, QD-625-Ab and QD-705-Ab respectively. The observed mean fluorescence intensity for QD-525-Ab conjugate was 84.98 ± 2.09, while for QD-625-Ab and QD-705-Ab conjugates the observed levels were 30.92 ± 0.83 and 98.08 ± 0.13 respectively (Fig. 3a).

Furthermore, we checked the applicability of immuno-conjugates to detect the molecular signatures in plasma samples. The mean fluorescence intensity indicating the detection of signatures in the plasma samples (0.22 μm filtered) was 4.62 ± 0.45%, 0.50 ± 0.05% and 2.35 ± 0.05% for QD-525-Ab, QD-625-Ab and QD-705-Ab immuno-conjugates respectively. Since the nucleic acids generally circulate as DNA-histone complexes, 0.22 μm filtration is likely to eliminate the large sized genetic debris resulting in minimal levels of fluorescence. While, the samples subjected to filtration by 0.45 μm filters removed extracellular microvesicles, lipid rafts, apoptotic/necrotic bodies and exosomes, conserving the nucleosomes (DNA-histone complexes), methylated *ccf*-DNA and AGO2-bound *ccf*-miRs. Upon analysis of the targets in 0.45 μm filtered plasma, we observed significantly higher fluorescence intensity in all three analyzed immuno-conjugates. The levels were 43.36 ± 1.07, 14.40 ± 0.61, and 46.39 ± 5.66 for QD-525-Ab, QD-625-Ab and QD-705-Ab immuno-conjugates respectively (Figs. 3b and 4). The shift in the fluorescence intensity observed could be attributed to the changes in the chemical environment of the QD-Ab conjugates. When they encounter with the target analytes, quantum confinement state might also change due alteration in QD size/shape [41–43]. The above results clearly demonstrate the ability of prepared QD-Ab immuno-conjugates to effectively capture and detect respective molecular signatures in plasma samples.

The capability of detection of individual epigenomic signatures at varying concentration (10 ng–0.001 ng) was assessed in 0.22 μm filtered plasma samples spiked with reference controls. A positive co-relation of the fluorescence intensity with the target analytes was observed in plasma samples spiked with of varying concentrations of reference controls (10 ng–0.001 ng). From the flow cytometry data, it was evident that the prepared triple QD-Ab conjugate could precisely recognize the target analytes upto 0.001 ng (Fig. 5a). In corroboration, fluorometry results also confirmed a similar trend (Fig. 5b). The trend observed in spiked samples with the reference controls confirmed the high efficacy and detection capability of the QD-Ab conjugates for specific determination of the molecular marks in circulation. However, an important point here is that the patterns of epigenetic modifications may significantly vary at individual levels. As the quantity of these signatures varies significantly within cells and tissues of an individual, the assay may be highly useful to determine the levels of differences of each epi-marks present in the circulating milieu.

After, establishing the ability of the prepared immuno-conjugates in detection of individual signatures, we further assessed the potential of these triple QD-Ab immuno-conjugates to function as a single tube assay format for simultaneous detection of the all three epi-marks. During concurrent detection spectral interference and/or overlapping may be an imminent issue. The QDs with unique fluorescence properties offer

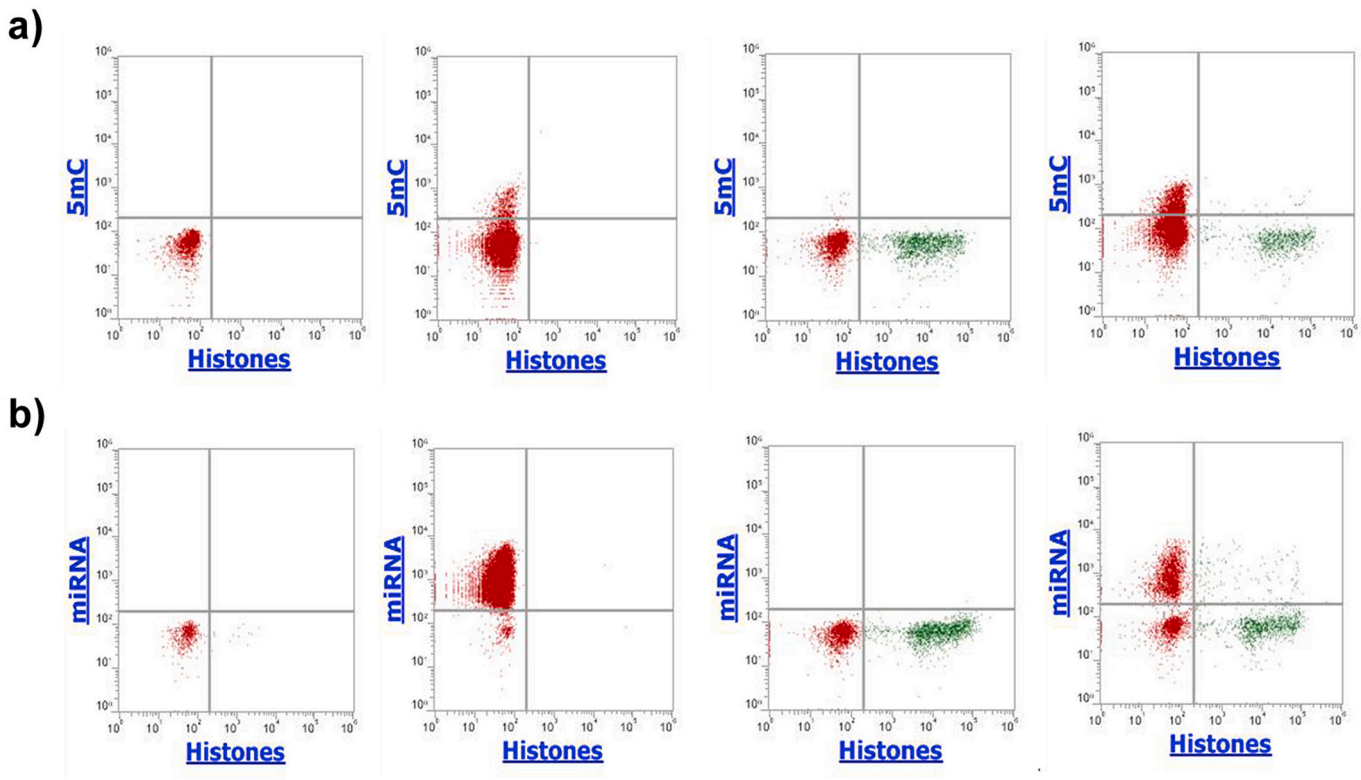

Fig. 6. Representative dot plot demonstrating the concurrent flow cytometric detection of circulating H3 histones with tri-methylation at the lysine 4, 9, 27 and 36 sites, methylation at the 5th carbon of cytosine of *ccf*-DNA and AGO2 bound *ccf*-miRs by the respective QD-Ab immuno-conjugates. The lower left quadrant was set to the double negative population while lower right represents acquired populations positive only for the fluorescence of x axis. The upper left and upper right quadrants denote the population positive for y axis and double positive respectively.

significant advantages in such multicolor applications, as they possess narrow emission spectra that lead to minimal overlap. Moreover, the process of compensation further reduces the spillover fluorescence by estimating its magnitude as a fraction of the measured fluorescence in the primary detector. In our experiments, we observed a minimal spectral overlap between all three prepared conjugates along with an excellent sensitivity. In addition, for simultaneous detection enriched samples were mixed (histones: methylated *ccf*-DNA and histones: AGO2 bound *ccf*-miRs) and analyzed. We analyzed the samples using combinations of two reporter conjugates by flow cytometry. The first immuno-sensing reporter cocktail comprised of QD-525-Ab and QD-625-Ab conjugates, showed the levels of H3 histones with tri-methylation at the lysine 4, 9, 27 and 36 sites and *ccf*-DNA consisting of methyl group attached at the 5th carbon of cytosine, simultaneously. While, the second immuno-sensing reporter cocktail consisted of QD-525-Ab and QD-705-Ab conjugates, indicated the levels of tri-methylated H3 histones and AGO2-bound *ccf*-miRs present in the samples. Owing to the different optical properties of three QDs, analyses were performed using three different channels of the flow cytometry. For comparative analysis, Ab conjugated QDs (QD-525-Ab, QD-625-Ab and QD-705-Ab) were utilized as negative control. The results exhibited high efficacy of the reporter cocktail to simultaneously detect their respective targets (Fig. 6). The upper left and lower right quadrant of the flow cytometry dot plots clearly indicates the signals positive for the respective target analytes i.e. tri-methylated H3 histone tails, methylated cytosine of *ccf*-DNA or AGO-bound *ccf*-miRs. The observations confirmed the applicability of the developed triple sensing immunoassay for simultaneous real-time recognition of the triple epigenomic signatures. Based on an individual's epigenetic landscape, the assay as a screening approach might help in detection and monitoring of the aberrant expression of epigenomic signatures that serves as surrogate markers for diagnosis of a disease at the early stages. The present work emphasized the detection of all the three epigenomic markers in a single tube format as an efficient strategy that might help to predict the onset and development of non-communicable diseases accompanied by lifestyle changes, thereby reducing the health burden.

4. Conclusion

Over the past few years, circulating epigenetic signatures such as methylated DNA, post-translationally modified histones and miRNAs have gathered significant attention. The high stability and differential expression of these biological moieties in normal and disease states offer their use as marker for gaining real-time information of an individual's health. However, considerable heterogeneity and unavailability of a sensitive method limits the use of these markers in clinics. With the advancement in the field of sensing, novel nano-material based portable biosensors may assist in providing sensitive and multiplexed detection of these circulating bio-molecules. The present work describes a unique "mix and measure" concurrent cytometric-assay for real-time assessment of cell free circulating epigenomic bio-molecules using a combination of three nano-sized semi-conducting nanocrystal based immuno-constructs in a single reporter cocktail. The amalgamation of the high affinity of Ab-antigen complex with the precision of flow cytometry offers accurate, specific and highly sensitive detection approach. After appropriate validation in clinical and field settings, the assay might prove beneficial to characterize aberrant circulating epigenetic signatures in various diseased conditions. In addition, the assay may also be utilized to monitor the lifestyle and environmental induced changes on human epigenomic landscape.

Authors' contributions

PKM devised the concept of research, and supervised the

experiments; RS, NB and RK performed the conjugation procedures; NB and RK executed PCR assays and performed ELISA and Western blot experiments; AB and PKM performed flow cytometry and analyzed results; KC and IYG helped in data analysis and interpretation; RS, AB and PKM wrote the manuscript.

Declaration of competing interest

The authors declare that they have no known competing financial interests or personal relationships that could have appeared to influence the work reported in this paper.

Acknowledgements

The authors are thankful to the Indian Council of Medical Research, Ministry of Human Resource and Development, Government of India, New Delhi (India) and Russian Foundation for Basic Research, Moscow (Russian Federation) for funding support to the laboratory of Professor Pradyumna Kumar Mishra. The technical support received from Mr. Pushpendra Kumar Gupta is gratefully acknowledged.

Appendix A. Supplementary data

Supplementary data to this article can be found online at https://doi.org/10.1016/j.talanta.2020.121516.

References

[1] M. Laura Soriano, M. Zougagh, M. Valcárcel, A. Ríos, Analytical Nanoscience and Nanotechnology: where we are and where we are heading, Talanta 177 (2018) 104–121, https://doi.org/10.1016/j.talanta.2017.09.012.
[2] R. Shandilya, A. Bhargava, N. Bunkar, R. Tiwari, I.Y. Goryacheva, P.K. Mishra, Nanobiosensors: point-of-care approaches for cancer diagnostics, Biosens. Bioelectron. 130 (2019) 147–165, https://doi.org/10.1016/j.bios.2019.01.034.
[3] R. Shandilya, A.M. Sobolev, N. Bunkar, A. Bhargava, I.Y. Goryacheva, P.K. Mishra, Quantum dot nanoconjugates for immuno-detection of circulating cell-free miRNAs, Talanta 208 (2020) 120486, https://doi.org/10.1016/j.talanta.2019.120486.
[4] A. Tadimety, A. Syed, Y. Nie, C.R. Long, K.M. Kready, J.X. Zhang, Liquid biopsy on chip: a paradigm shift towards the understanding of cancer metastasis, Integr Biol (Camb). 9 (1) (2017) 22–49, https://doi.org/10.1039/c6ib00202a.
[5] B. Mathew, A. Alazzam, S. Khashan, M. Abutayeh, Lab-on-chip for liquid biopsy (LoC-LB) based on dielectrophoresis, Talanta 164 (2017) 608–611, https://doi.org/10.1016/j.talanta.2016.11.008.
[6] W. Gao, T. Huang, H. Yuan, J. Yang, Q. Jin, C. Jia, G. Mao, J. Zhao, Highly sensitive detection and mutational analysis of lung cancer circulating tumor cells using integrated combined immunomagnetic beads with a droplet digital PCR chip, Talanta 185 (2018) 229–236, https://doi.org/10.1016/j.talanta.2018.03.083.
[7] A. Gharatape, A.Y. Khosroushahi, Optical biomarker-based biosensors for cancer/infectious disease medical diagnoses, Appl. Immunohistochem. Mol. Morphol. 27 (4) (2019) 278–286, https://doi.org/10.1097/PAI.0000000000000586.
[8] C.S. Huertas, O. Calvo-Lozano, A. Mitchell, L.M. Lechuga, Advanced evanescent-wave optical biosensors for the detection of nucleic acids: an analytic perspective, Front Chem 7 (2019) 724, https://doi.org/10.3389/fchem.2019.00724.
[9] P. Damborský, J. Švitel, J. Katrlík, Optical biosensors, Essays Biochem. 60 (1) (2016) 91–100, https://doi.org/10.1042/EBC20150010.
[10] O.A. Goryacheva, A.S. Novikova, D.D. Drozd, P.S. Pidenko, T.S. Ponomaryeva, A. A. Bakal, P.K. Mishra, N.V. Beloglazova, I.Y. Goryacheva, Water-dispersed luminescent quantum dots for miRNA detection, TrAC Trends Anal. Chem. (Reference Ed.) 111 (2019) 197–205, https://doi.org/10.1016/j.trac.2018.12.022.
[11] H. Feng, Z. Qian, Functional carbon quantum dots: a versatile platform for chemosensing and biosensing, Chem. Rec. 18 (5) (2018) 491–505, https://doi.org/10.1002/tcr.201700055.
[12] O.A. Goryacheva, P.K. Mishra, I.Y. Goryacheva, Luminescent quantum dots for miRNA detection, Talanta 179 (2018) 456–465, https://doi.org/10.1016/j.talanta.2017.11.011.
[13] I. Mittra, N.K. Nair, P.K. Mishra, Nucleic acids in circulation: are they harmful to the host? J. Biosci. 37 (2) (2012) 301–312, https://doi.org/10.1007/s12038-012-9192-8.
[14] S. Filipów, Ł. Łaczmański, Blood circulating miRNAs as cancer biomarkers for diagnosis and surgical treatment response, Front. Genet. 10 (2019) 169, https://doi.org/10.3389/fgene.2019.00169.
[15] J.C. Yeo, C.T. Lim, Potential of circulating biomarkers in liquid biopsy diagnostics, Biotechniques 65 (4) (2018) 187–189, https://doi.org/10.2144/btn-2018-0093.
[16] J. Das, S.O. Kelley, High-performance nucleic acid sensors for liquid biopsy applications, Angew Chem. Int. Ed. Engl. 59 (7) (2020) 2554–2564, https://doi.org/10.1002/anie.201905005.
[17] A. Kustanovich, R. Schwartz, T. Peretz, A. Grinshpun, Life and death of circulating cell-free DNA, Canc. Biol. Ther. 20 (8) (2019) 1057–1067, https://doi.org/10.1080/15384047.2019.1598759.
[18] J. E Kim, N. Lee, J.Y. Gu, H.J. Yoo, H.K. Kim, Circulating levels of DNA-histone complex and dsDNA are independent prognostic factors of disseminated intravascular coagulation, Thromb. Res. 135 (6) (2015) 1064–1069, https://doi.org/10.1016/j.thromres.2015.03.014.
[19] D. Völler, L. Linck, A. Bruckmann, J. Hauptmann, R. Deutzmann, G. Meister, A. K. Bosserhoff, Argonaute family protein expression in normal tissue and cancer entities, PloS One 11 (8) (2016), e0161165, https://doi.org/10.1371/journal.pone.0161165.
[20] A. Turchinovich, T.R. Samatov, A.G. Tonevitsky, B. Burwinkel, Circulating miRNAs: cell-cell communication function? Front. Genet. 4 (2013) 119, https://doi.org/10.3389/fgene.2013.00119.
[21] J.Y. Leung, K. Chia, D.S.T. Ong, R. Taneja, Interweaving tumor heterogeneity into the cancer epigenetic/metabolic axis, Antioxidants Redox Signal. (2019 Dec 16), https://doi.org/10.1089/ars.2019.7942.
[22] A.L. Volckmar, H. Sültmann, A. Riediger, T. Fioretos, P. Schirmacher, V. Endris, A. Stenzinger, S. Dietz, A field guide for cancer diagnostics using cell-free DNA: from principles to practice and clinical applications, Genes Chromosomes Cancer 57 (3) (2018 Mar) 123–139, https://doi.org/10.1002/gcc.22517.
[23] J. Marrugo-Ramírez, M. Mir, J. Samitier, Blood-based cancer biomarkers in liquid biopsy: a promising non-invasive alternative to tissue biopsy, Int. J. Mol. Sci. 19 (10) (2018), https://doi.org/10.3390/ijms19102877 pii: E2877.
[24] I.B. Hench, J. Hench, M. Tolnay, Liquid biopsy in clinical management of breast, lung, and colorectal cancer, Front. Med. 5 (2018) 9, https://doi.org/10.3389/fmed.2018.00009.
[25] R. Palmirotta, D. Lovero, P. Cafforio, C. Felici, F. Mannavola, E. Pellè, D. Quaresmini, M. Tucci, F. Silvestris, Liquid biopsy of cancer: a multimodal diagnostic tool in clinical oncology, Ther Adv Med Oncol 10 (2018), https://doi.org/10.1177/1758835918794630, 1758835918794630.
[26] S.A. Zaidi, F. Shahzad, S. Batool, Progress in cancer biomarkers monitoring strategies using graphene modified support materials, Talanta 210 (2020) 120669, https://doi.org/10.1016/j.talanta.2019.120669.
[27] A. Ebrahimi, I. Nikokar, M. Zokaei, E. Bozorgzadeh, Design, development and evaluation of microRNA-199a-5p detecting electrochemical nanobiosensor with diagnostic application in Triple Negative Breast Cancer, Talanta 189 (2018) 592–598, https://doi.org/10.1016/j.talanta.2018.07.016.
[28] N. M Noah, P.M. Ndangili, Current trends of nanobiosensors for point-of-care diagnostics, J Anal Methods Chem 2019 (2019) 1–16, https://doi.org/10.1155/2019/2179718.
[29] O.A. Goryacheva, A.M. Vostrikova, A.A. Kokorina, E.A. Mordovina, D.V. Tsupka, A. A. Bakal, R. Shandilya, P.K. Mishra, N.V. Beloglazova, I.Y. Goryacheva, Luminescent carbon nanostructures for microRNA detection, Trends Anal. Chem. 119 (2019) 115613, https://doi.org/10.1016/j.trac.2019.07.024.
[30] G. Greub, R. Sahli, R. Brouillet, K. Jaton, Ten years of R&D and full automation in molecular diagnosis, Future Microbiol. 11 (3) (2016) 403–425, https://doi.org/10.2217/fmb.15.152.
[31] F. Di Nardo, L. Anfossi, C. Giovannoli, C. Passini, V.V. Goftman, I.Y. Goryacheva, C. Baggiani, A fluorescent immunochromatographic strip test using Quantum Dots for fumonisins detection, Talanta 150 (2016) 463–468, https://doi.org/10.1016/j.talanta.2015.12.072.
[32] A. Bhargava, N. Pathak, S. Seshadri, N. Bunkar, D.K. Mishra, N.K. Lohiya, P. K. Mishra, Pre-clinical validation of mito-targeted nano-engineered flavonoids isolated from selaginella bryopteris (sanjeevani) as A novel cancer prevention strategy, Anticancer Agents Med Chem 18 (2018) 1860–1874, https://doi.org/10.2174/1871520618666171229223919.
[33] N. Bunkar, A. Bhargava, K. Chaudhury, R.S. Sharma, N.K. Lohiya, P.K. Mishra, Fetal nucleic acids in maternal plasma: from biology to clinical translation, Front. Biosci. 23 (2018) 397–431, https://doi.org/10.2741/4597.
[34] A. Shukla, N. Bunkar, R. Kumar, A. Bhargava, R. Tiwari, K. Chaudhury, I. Y. Goryacheva, P.K. Mishra, Air pollution associated epigenetic modifications: transgenerational inheritance and underlying molecular mechanisms, Sci. Total Environ. 656 (2019) 760–777, https://doi.org/10.1016/j.scitotenv.2018.11.381.
[35] A. Bhargava, N.K. Khare, N. Bunkar, K. Chaudhury, K.C. Pandey, S.K. Jain, P. K. Mishra, Cell-free circulating epigenomic signatures: non-invasive biomarker for cardiovascular and other age-related chronic diseases, Curr. Pharmaceut. Des. 28 (2017) 1175–1187, https://doi.org/10.2174/1381612822666161027145359.
[36] T.D. Becke, S. Ness, S. Sudhop, H.E. Gaub, M. Hilleringmann, A.F. Schilling, H. Clausen-Schaumann, Covalent immobilization of proteins for the single molecule force spectroscopy, JoVE 138 (2018), https://doi.org/10.3791/58167.
[37] A.K. Trilling, J. Beekwilder, H. Zuilhof, Antibody orientation on biosensor surfaces: a minireview, Analyst 138 (6) (2013) 1619–1627, https://doi.org/10.1039/c2an36787d.
[38] D. Lou, L. Ji, L. Fan, Y. Ji, N. Gu, Y. Zhang, Antibody-oriented strategy and mechanism for the preparation of fluorescent nanoprobes for fast and sensitive immunodetection, Langmuir 35 (14) (2019) 4860–4867, https://doi.org/10.1021/acs.langmuir.9b00150.
[39] G. Ruiz, K. Tripathi, S. Okyem, J.D. Driskell, pH impacts the orientation of antibody adsorbed onto gold nanoparticles, Bioconjugate Chem. 30 (4) (2019) 1182–1191, https://doi.org/10.1021/acs.bioconjchem.9b00123.
[40] S. Pathak, M.C. Davidson, G.A. Silva, Characterization of the functional binding properties of antibody conjugated quantum dots, Nano Lett. 7 (7) (2007) 1839–1845, https://doi.org/10.1021/nl062706i.
[41] T.V. Torchynska, Physical Reasons of Emission Varying in CdSe/ZnS and CdSeTe/ZnS Quantum Dots at Bioconjugation to Antibodies, Quantum Dots - Theory and

Applications, Vasilios N. Stavrou, BT - Quantum Dots SP - Ch, vol. 6, IntechOpen, September 17th 2015, pp. 151–179, https://doi.org/10.5772/60821.

[42] T.V. Torchynska, G. Polupan, L.G. Vega Macotela, Emission transformation in CdSe/ZnS quantum dots conjugated to biomolecules, J. Photochem. Photobiol., B 170 (2017) 309–313, https://doi.org/10.1016/j.jphotobiol.2017.04.012.

[43] S. Dwarakanath, J.G. Bruno, A. Shastry, T. Phillips, A.A. John, A. Kumar, L. D. Stephenson, Quantum dot-antibody and aptamer conjugates shift fluorescence upon binding bacteria, Biochem. Biophys. Res. Commun. 325 (3) (2004) 739–743, https://doi.org/10.1016/j.bbrc.2004.10.099.